Journal of Alloys and Compounds 480 (2009) 843–848

Contents lists available at ScienceDirect

Journal of Alloys and Compounds

journal homepage: www.elsevier.com/locate/jallcom

Coprecipitation synthesis and thermal conductivity of $La_2Zr_2O_7$

Hongfei Chen[a,b], Yanfeng Gao[a,*], Yun Liu[a,b], Hongjie Luo[a]

[a] Shanghai Institute of Ceramics (SIC), Chinese Academy of Sciences (CAS), 1295 Dingxi, Changning, Shanghai 200050, China
[b] Graduate University of Chinese Academy of Sciences, 19 Yuquanlu, Beijing 100049, China

ARTICLE INFO

Article history:
Received 27 November 2008
Received in revised form 11 February 2009
Accepted 14 February 2009
Available online 4 March 2009

Keywords:
Lanthanum zirconate
Dropping order
Coprecipitation
Ceramic
Thermal conductivity

ABSTRACT

Lanthanum zirconate ($La_2Zr_2O_7$, LZ) was synthesized by a coprecipitation–calcination method with different dropping orders for the raw materials. We investigated synthesis procedures, including the chemical compositions of precipitate mixtures, the calcination process and the phase composition at different calcination temperatures. Simultaneous thermogravimetric and differential thermal analysis (TG–DTA) results of the mixtures show two different calcination processes for precipitates by the natural dropping and reverse dropping methods. Reactions starting in a basic solution (the reverse dropping method) can precipitate La and Zr ions simultaneously and form a –La–O–Zr– composite, resulting in a homogeneous composition on a molecular scale, and pure, high-crystalline LZ powders after calcination. When starting from an acid solution (the natural dropping method), the precipitate was a mixture of lanthanum hydroxide and zirconium hydroxide. Consequently, the final product was LZ with impurities. The overall thermal conductivity of LZ obtained by the reverse dropping method was about 50% lower than that by the natural dropping method.

1. Introduction

Advanced gas-turbines are being developed for high operating temperatures in order to increase thermal efficiency. Hot section components working in the combustion system must meet the rigorous requirements for extreme conditions, such as high temperature, thermal stress, thermal shock and severe corrosion [1–4]. The application of thermal barrier coatings (TBCs) can result in a large temperature decrease between the hot gas and the metal substrate. State-of-the-art TBC is currently made of yttria-stabilized zirconia (YSZ) [5–7]. However, a major disadvantage of YSZ is its limited operation temperature (1200 °C) for long-term application [8]. Recently, lanthanum zirconate (LZ), a novel candidate for next generation TBC ceramic materials, has attracted much interest due to its low thermal conductivity, high melting point (2280 °C), high sintering-resistance and phase stability [9–12].

The performance of TBCs depends largely on the synthesis procedures and conditions. Different methods, including solid-state reaction, solution routes using organic and inorganic precursors, and hydrothermal synthesis [5,13–15], can be used to prepare LZ with various sizes, morphologies and crystalline properties. The coprecipitation–calcination method [16] is an easy, effective method to obtain tiny precursor particles that are needed for fabricating TBCs with a fine structure and a low thermal diffusivity. Grain boundaries are favorable for increasing the scatter probability of phonons, leading to a low thermal conductivity and enhanced thermal cycling resistance [17].

Although the coprecipitation–calcination method was employed to synthesize LZ, little attention has been paid to this procedure. If more effort is put into investigating the synthesis procedure, we will better understand the parameters, such as hydrolysis-complex reactions, calcination time and temperatures, all of which affect the quality of the final powders, such as phase compositions, particle sizes and morphologies. An increase in the quality of powders is of special importance to the subsequent preparation of TBCs and their performance. Coatings fabricated via the solution precursor plasma spray and air plasma spray (APS) usually show the same phase composition, but the microstructure and thermophysical properties are remarkably different because of the different feedstock [18,19]. Even employing the same process, APS, to prepare TBCs, using powders produced by different methods causes the performance of the TBCs to vary remarkably. The design of starting powders, including their crystalline phases, particle sizes, morphologies and surface physical chemistry, is crucial for improving the properties of coatings.

In a typical coprecipitation process, several solutions may be involved, usually including precursor solutions containing Zr^{4+} and La^{3+} and a precipitate agent, such as ammonium hydrate. Adding ammonium hydrate to a mixture solution of Zr^{4+} and La^{3+} (hereafter termed the natural dropping method) or adding the latter solution to the former one (the reverse dropping method) may support different hydrolysis-complex conditions. The natural

* Corresponding author. Tel.: +86 21 5241 5270; fax: +86 21 5241 5270.
E-mail address: yfgao@mail.sic.ac.cn (Y. Gao).

0925-8388/$ – see front matter © 2009 Elsevier B.V. All rights reserved.
doi:10.1016/j.jallcom.2009.02.081

dropping method occurs in an initial acidic reaction environment that subsequently changes slowly to basic, whereas the reverse dropping method occurs in a constant strong basic reaction environment. These different reaction environments can alter the hydrolysis-complex processes, resulting in changes in morphology, size, crystalline phase and even the chemical composition of the final precipitates. Using two opposite dropping methods, Kawano and Imai [20] selectively synthesized ZnO spherical grains and rods with various aspect ratios in an aqueous system. It was believed that the selection of the preparation routes was essential for the control of the morphology of ZnO particles. Furthermore, the different dropping methods can also affect the size of the final products [21]. If the coprecipitation mechanism was well understood, such as how coprecipitation develops using these two methods and the dominant factors therein, we could prepare high-quality powders with optimized particle size and morphology.

This study aims to investigate the formation mechanism of the coprecipitation–calcination process by studying in detail how the two methods affect the morphology of LZ powders and the crystallization process during calcination. The LZ ceramics were produced, and their thermal conductivities were measured.

2. Experimental

2.1. Powder synthesis and specimen preparation

In this study, lanthanum nitrate ($La(NO_3)_3{\cdot}6H_2O$), zirconium oxychloride ($ZrOCl_2{\cdot}8H_2O$) and ammonium hydrate ($NH_3{\cdot}H_2O$) were chosen as reactants. All chemicals used in this study were analytical-grade from Shanghai Chemical Regent Co., China. Lanthanum nitrate and zirconium oxychloride were separately dissolved in deionized water with proper molar amounts. The concentration of both solutions was 0.1 M. Then, two solutions were mixed. After stirring for about 30 min, two methods, the natural dropping and reverse dropping were carried out with stirring. The rate of dropping was about 30 drops min^{-1}. The same amount of ammonium hydrate solution was used in two methods. After reaction, gel-like precipitates were obtained, subsequently filtered and washed with deionized water three times. Then the washed precipitates were dried at 110 °C for 4 h and ball-milled. Calcinations were carried out at different temperatures ranging from 500 °C to 1000 °C in air for 4 h. Finally, the products were milled into fine powder.

The powder used for specimen fabrication was synthesized by the reverse dropping method. Specimens for the determination of thermal diffusivity were prepared by uniaxially cold pressing at 80 MPa. The green body was then sintered at 1500 °C in air for 6 h to yield disc-shaped specimen about 11 mm in diameter and 0.8 mm in thickness.

2.2. Characterization techniques

The phase compositions of the powders were determined by X-ray diffraction (XRD, Rigaku RINT2200) using Cu Kα radiation. The bulk density of the specimen was measured by the Archimedes method with an immersion medium of deionized water. Transmission electron microscopy (TEM) images were taken by a JEM-2010 transmission electron microscope (Tokyo, Japan) equipped with an energy dispersive spectrometer (EDS).

Simultaneous thermogravimetric (TG) and differential thermal analysis (DTA) were performed in air using a Polymer Lab. Thermal Science System, with platinum cups as sample holders. The thermal analysis experiments were performed at a heating rate of 10 K min^{-1}. The thermal diffusivity of the sintered sample was measured, using the laser-flash method, as a function of specimen temperature (in the range between 200 °C and 1200 °C) in an argon atmosphere. For thermal diffusivity measurement, both the front and back faces of the specimen were coated with a thin layer of graphite, which can prevent the laser beam from direct transition through the specimen.

3. Results and discussion

3.1. Procedure studies of the coprecipitation–calcination method

3.1.1. Chemical compositions of as-prepared precipitate mixtures

Stable zirconium hydroxide precipitate can be formed at about pH 4.5 [22], while $La(NO_3)_3$ begins to form stable precipitates at about pH 8.35 [23]. In the precipitation process, the pH value of the solution varied from 0.6 to 10 with the addition of ammonium hydrate using the natural dropping method. Precipitation can be regarded as a process of cations scrambling for OH^- in solution. When pH < 8.35, Zr^{4+} is better than La^{3+} in the ability to combine with OH^-. Therefore, through the natural dropping method, a zirconium hydroxide precipitate is formed first. When the pH value attains about 8.35, a majority of Zr^{4+} has already been precipitated and La^{3+} begins to combine with OH^- to form a precipitate gel. Thus, the precipitates obtained by this method are more likely to be a mechanical mixture of zirconium and lanthanum hydroxide rather than a real "coprecipitation". However, when using the reverse dropping method, the pH value decreases from 13 to 10 after reactions, and the amount of OH^- is in excess for the formation of Zr^{4+} and La^{3+} precipitates. Zr^{4+} and La^{3+} can coprecipitate simultaneously (Fig. 1). Moreover, in terms of a quantitative analysis of EDS (Table 1), where five spots on different parts of the precipitate were measured, the molar ratio of La/Zr/O is about 1/1/1. Accordingly, the precipitate may possess a network structure like –La–O–Zr–, which can also be proven by the TG–DTA analysis (see below for details). On the other hand, an amorphous precipitate obtained by the natural dropping method was a mixture of zirconium and lanthanum hydroxide (spot 1 to spot 4 is shown in Table 2). In addition, some "rods" were observed to have dispersed among the precipitate. These rods may be lanthanum oxide or hydroxide (spot 5 in Table 2), in good agreement with the results that show that the amount of La is slightly less than Zr (spot 1 to spot 4 in Table 2).

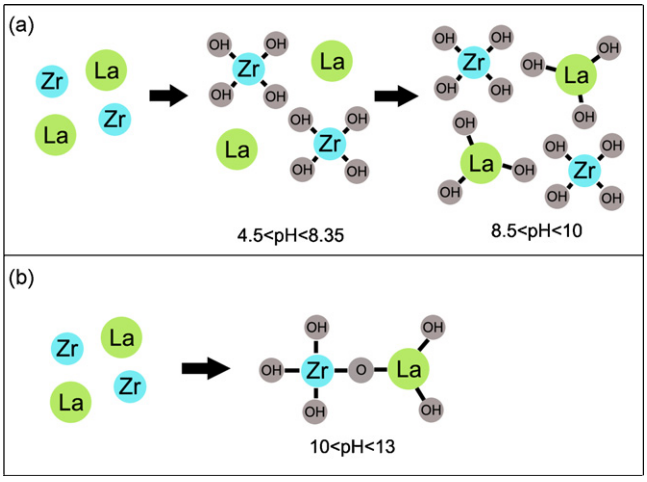

Fig. 1. Schematic diagram of coprecipitation by two methods: (a) the natural dropping method; (b) the reverse dropping method.

Table 1
EDS results of precipitate obtained by the reverse dropping method (molar ratio; measurement spots shown as a cross in Fig. 2).

Element	Spot 1	Spot 2	Spot 3	Spot 4	Spot 5
O	38.50	37.42	35.36	37.21	38.12
Zr	31.33	32.05	32.52	31.36	31.53
La	30.16	30.53	32.12	31.42	30.35

3.1.2. Morphologies of precipitate mixtures

The morphologies of the precipitates were observed by TEM (Fig. 4). The majority of precipitate gels obtained by both methods

Table 2
EDS results of precipitate obtained by the natural dropping method (molar ratio; measurement spots shown as a cross in Fig. 3).

Element	Spot 1	Spot 2	Spot 3	Spot 4	Spot 5
O	65.35	68.94	68.12	67.68	38.12
Zr	19.37	18.42	17.65	18.96	1.31
La	15.28	12.64	14.22	13.36	60.56

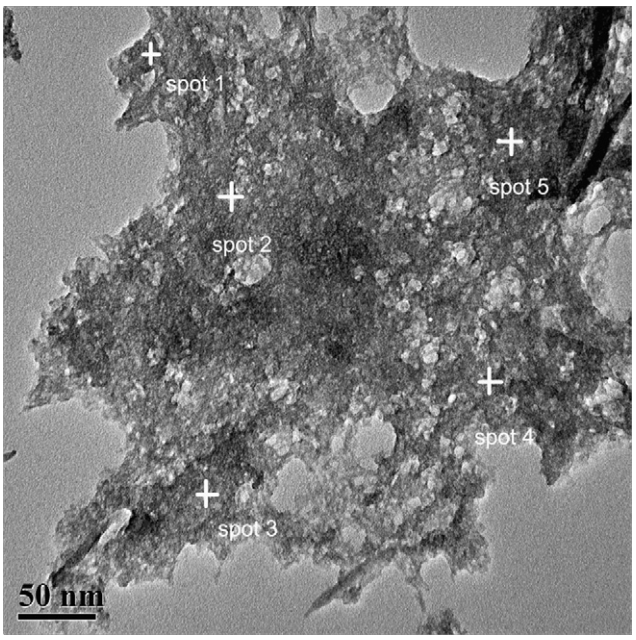

Fig. 2. TEM image of as-prepared precipitate by the reverse dropping method.

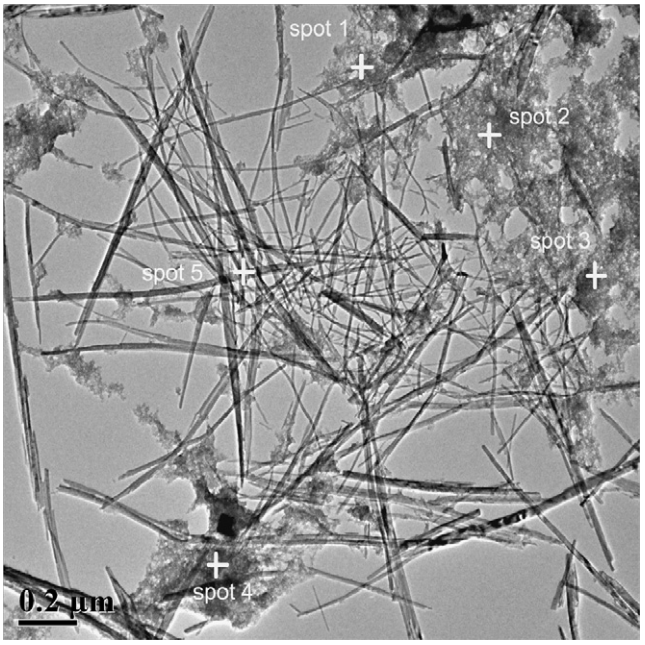

Fig. 3. TEM image of as-prepared precipitate by the natural dropping method.

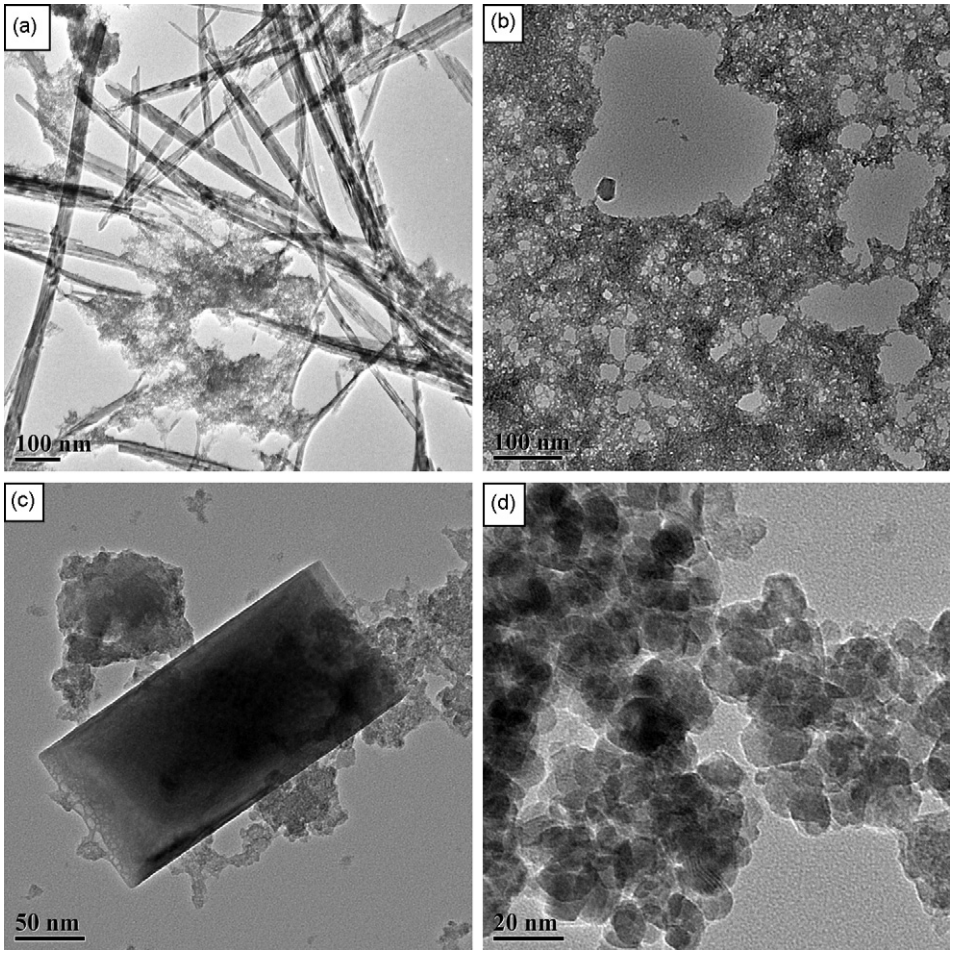

Fig. 4. TEM images of precipitate gel prepared by the natural dropping method (a and c) and by the reverse dropping method (b and d) before (a and b) and after (c and d) drying.

are amorphous. The gel particles prepared by the reverse dropping method (Fig. 4b) seem to be more uniform and smaller than those prepared by the natural dropping method (Fig. 4a). Both precipitates consist of needle-shaped particles. However, some large rod-shaped ones can also be seen with the natural dropping method (Fig. 4a). After drying at 110 °C for 4 h, the rod-shaped particles (Fig. 4a) disappeared, and replaced by a small amount of rectangular crystals (Fig. 4c). The precipitate from the reverse dropping method developed into large spherical particles (Fig. 4d). The presence of rod-like particles and rectangular crystals is unexpected, since no crystal phases were observed in XRD patterns at such low temperatures. According to EDS and electron diffraction results, these rods and rectangle crystals were a kind of lanthanum oxide or lanthanum hydroxide single crystal (Table 2, spot 5), whose presence can be ascribed to the fluctuation of energy in solution and the instability of the precipitate. Through the natural dropping method, the precipitates of Zr^{4+} and La^{3+} disperse heterogeneously, and no tight interconnections between them form. A relatively stable precipitate with the –La–O–Zr– networks can be formed by the reverse dropping method and the chemical bond binds the two cations together, which disables the lanthanum-related precipitates from aggregating to form large crystals. The great difference in product morphology from the two methods can be related to the structural evolution of zirconia sol–gels during the preparation. Under variant pH conditions, the hydrolyzing products of Zr^{4+} derived from diverse coordination chemistry can differ in the structure from each other [24]. Because the difference in pH value for the two methods, Zr^{4+} coordinated with both La^{3+} and OH^- in the reverse dropping method, nevertheless Zr^{4+} only coordinated with OH^- in the natural dropping method (Fig. 1). The difference in coordination structures on atom scale led to the microstructural differences in size and morphology. However, further studies are needed to investigate the relationship between coordination structure and morphologies, as well as the formation process of the particles.

3.1.3. XRD studies

The XRD profiles of precipitates by the reverse dropping method calcined at different temperatures are present in Fig. 5. It can be seen that below 700 °C, the product is almost amorphous. When the temperature is increased to 750 °C, peaks, such as (2 2 0), (4 0 0), and (4 4 0), can be recognized clearly in Fig. 5c, indicating the formation of a new phase. This phase should be lanthanum zirconate with a fluorite structure [25]. Increasing the temperature to 850 °C and 900 °C causes the diffraction peaks to become sharper. When

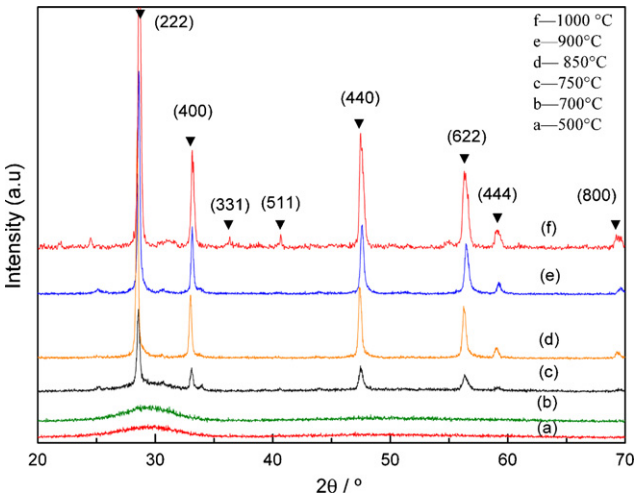

Fig. 5. XRD patterns of precipitate by the reverse dropping method calcined at different temperatures for 4 h.

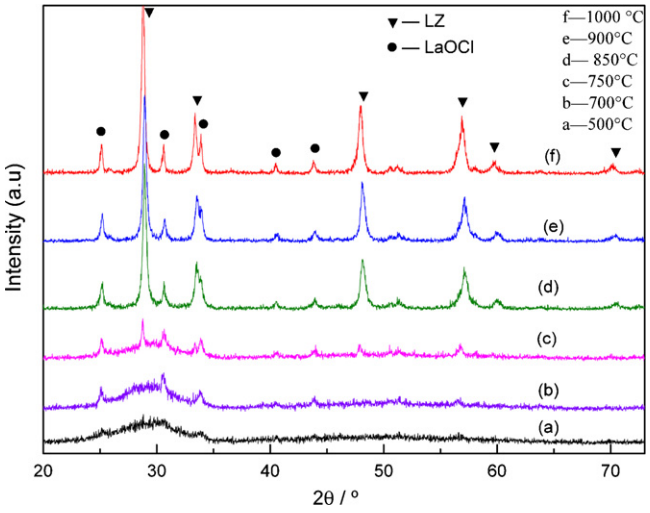

Fig. 6. XRD patterns of precipitate by the natural dropping method calcined at different temperatures for 4 h.

the temperature reaches 1000 °C (Fig. 5f), two small peaks (3 3 1) and (5 1 1) appear which cannot be seen at 900 °C. Generally, the existence of peaks such as (3 3 1), (5 1 1), (1 1 1) is used as a confirmation of the pyrochlore structure [26,27]. In addition, according to the standard XRD profile of $La_2Zr_2O_7$ (JCPDS Card No. 73-0444), it is believed that lanthanum zirconate with a pyrochlore structure is obtained at this temperature. Apparently, it is transformed from the fluorite phase. This synthesis temperature is much lower than that of solid-state reaction (1500 °C) [28], which is one advantage of the coprecipitation method in the preparation of complex oxides at low temperatures from ultra-fine precursor powders mixed uniformly at the molecular level. The grain size of the synthesized LZ, about 10 nm, was calculated by the Scherrer formula.

Fig. 6 shows the XRD patterns of the precipitate formed from the natural dropping method and calcined at different temperatures. Below 500 °C, the precipitate is amorphous, similar to the case of the reverse dropping method. At 700 °C, several small peaks can be observed, but cannot be assigned to LZ. In addition to the unexpected phase, from 750 °C to 1000 °C, the characteristic peaks of LZ (2 2 0), (4 0 0), and (4 4 0) also appear and become sharper with increasing temperature. At 1000 °C, the impure phase can be completely identified as LaOCl. The formation of this compound can result from the combination of lanthanum hydroxide (these needle-like particles) and Cl^- (see Table 3), which remains in solution even after washing three times.

In addition to the difference in the phase compositions of the powders prepared by the two methods, the differences also include the following characteristics. After calcination at a temperature above 750 °C for 4 h, the degree of crystallinity of the powders obtained by the reverse dropping method is obviously higher than those prepared by the natural dropping method (see Figs. 5 and 6).

The major components of the precipitate synthesized by the natural dropping method are zirconium hydroxide and lanthanum hydroxide, while a –La–O–Zr– compound was created by the reverse dropping method, as analyzed above. The La, Zr and O are more homogeneously dispersed in –La–O–Zr–. When calcined, the –La–O–Zr– compound transformed to LZ more smoothly. However, the hydroxides formed by the natural dropping method needed to transform to the corresponding oxides that subsequently react to form LZ. Note that some of the precipitates prepared by the natural dropping method can not form LZ particles completely, suggesting that the reverse dropping method is easier to control in terms of the stoichiometry.

Table 3
Chemical composition and crystallinity of products by the natural and reverse dropping methods.

Sample	La (at.%)	Zr (at.%)	Cl (at.%)	Composition	Purity (LZ)	Crystallinity
Natural	49.39	48.36	2.15	$0.977La_2O_3{\cdot}2ZrO_2$; LaOCl	97.13%	Polycrystal
Reverse	49.96	49.89	NF[a]	$1.001La_2O_3{\cdot}2ZrO_2$	99.91%	Single crystal

[a] Not find.

3.1.4. Thermal analysis

The TG–DTA results for the gel prepared by the natural dropping method are shown in Fig. 7. Before thermal analysis, the gel was dried at 110 °C for 4 h. The DTA curve shows an endothermic peak at around 126.6 °C, with a weight loss in the TG curve. This change arises from desorption of the adsorbed water.

With the increase of temperature, the weight loss continues, and two endothermic peaks at around 325 °C and 400 °C can be observed in the DTA curve. The two peaks can be attributed to the release of structural water from lanthanum hydroxide and zirconium hydroxide, respectively.

Above 500 °C, the weight loss continues gently. At about 502 °C, an endothermic peak in the DTA curve can be observed, probably due to the further release of structural water or the decomposition of some impure compounds, such as lanthanum oxychloride (Fig. 6), that may be formed during operations. The product can be conjectured to be a compound of La/Zr/O at this temperature, because in the XRD patterns in Fig. 6, from 500 °C to 700 °C, a broad peak is present, which may be a sign of the transformation to an intermediate state of LZ with the fluorite structure (F). At about 854 °C, there is an exothermic peak in the DTA curve with almost no weight loss in the TG curve. It indicates a crystallization transition from the amorphous La/Zr/O compound to LZ (F). The exothermic peak around 1050 °C suggests a phase transition from the fluorite structure to the more ordered pyrochlore (P) structure [25].

The TG–DTA curve of the gel produced by the reverse dropping method is different from that of the natural dropping method. As shown in Fig. 8, the most obvious difference is that no clear thermal effects can be seen in the range from 300 °C to 700 °C. The endothermic peak at 122.8 °C, accompanied by weight loss, indicates desorption of the physically absorbed water. The flat DTA curve in the region of 300–700 °C indicates that no structural changes occur at this stage. The sharp exothermic peak at around 874.5 °C can be attributed to the crystallization transition from –La–O–Zr– to LZ (F), and the relatively small exothermic peak at around 1045 °C suggests a phase transition from LZ (F) to LZ (P), which is in accordance with the XRD pattern in Fig. 5.

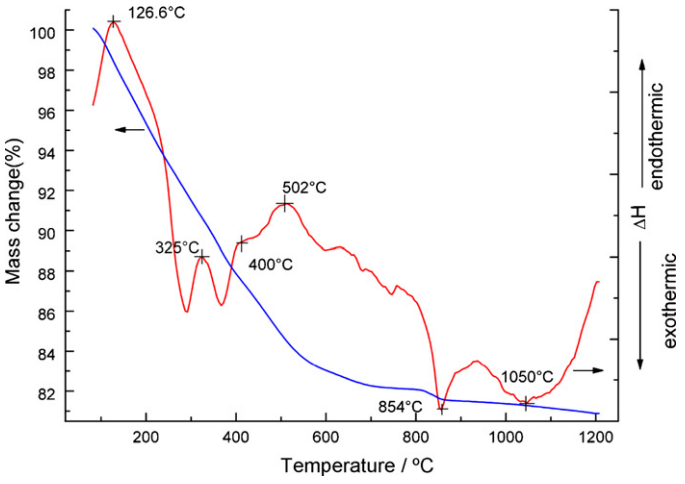

Fig. 7. TG–DTA traces of precipitate gel prepared by the natural dropping method.

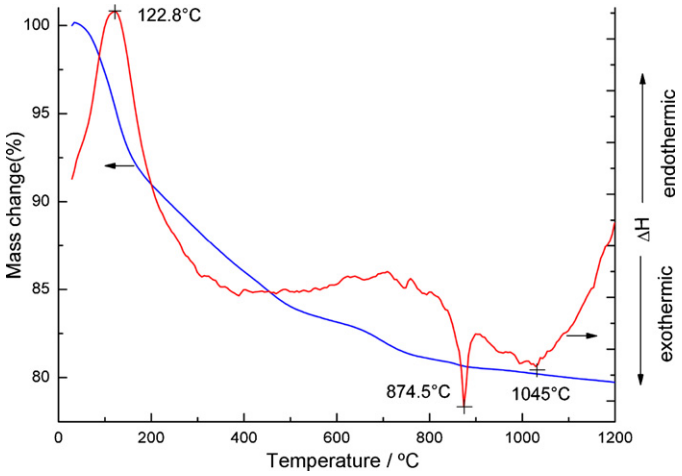

Fig. 8. TG–DTA traces of precipitate gel prepared by the reverse dropping method.

3.2. Thermophysical property

The specific heat values of $La_2Zr_2O_7$ at various temperatures are taken from the literature [29] and a density of 4.2 g cm^{-3} for both was measured by the Archimedes method. The values of thermal conductivity are then obtained by multiplying the thermal diffusivity (α), density (ρ) and specific heat (C_p), according to Eq. (1):

$$k = C_p \cdot \alpha \cdot \rho \quad (1)$$

The thermal diffusivity of $La_2Zr_2O_7$ decreases with increasing temperature in the range between 200 °C and 1200 °C (Fig. 9), suggesting an inverse temperature dependence (i.e. $\alpha \propto 1/T$). This change suggests a dominant phonon conduction behavior, which is found in most polycrystalline materials [30]. In the temperature range between 900 °C and 1200 °C, the thermal diffusivity decreases, while the thermal conductivity increases, which are

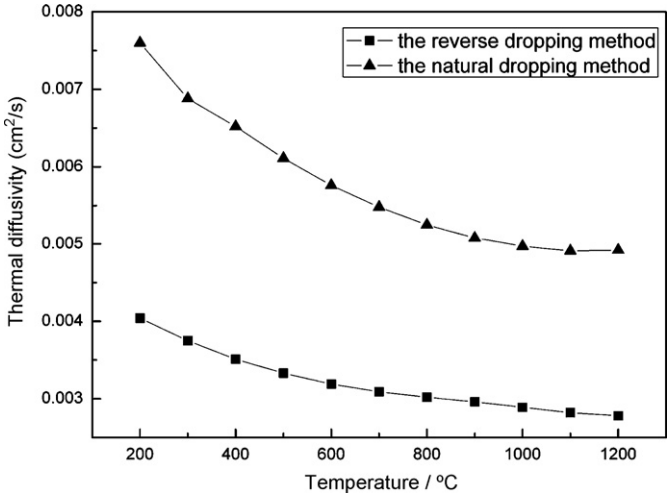

Fig. 9. Thermal diffusivity of LZ versus temperature by the natural and reverse dropping method.

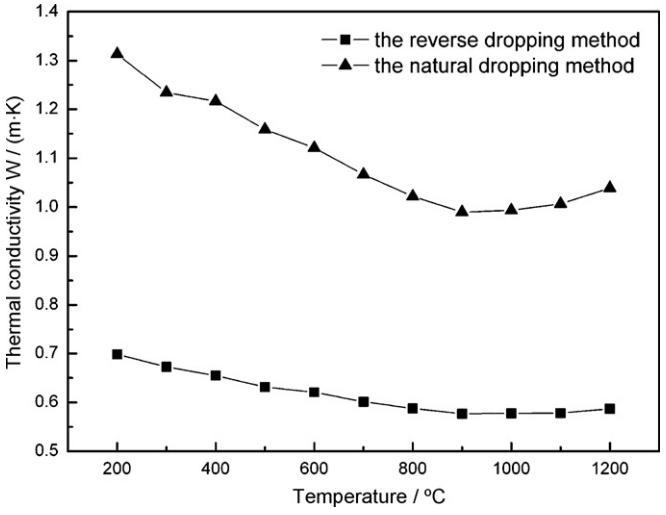

Fig. 10. Temperature dependence of thermal conductivity of LZ obtained by the natural and reverse dropping method.

shown in Fig. 10. It is attributed to the effects of thermal radiation at high temperature (>900 °C) [31].

The thermal conductivity of samples obtained with the reverse dropping method decreased by about a half compared to those produced by the natural dropping method, as shown in Fig. 10. The difference in the thermal property between two samples can be related to their compositions (Table 3), microstructure and the properties of the second phase. As analyzed in the former section, the sample obtained by the reverse dropping method is composed of pure LZ (P), while the sample produced by the natural dropping method contains a small amount of impure phase, LaOCl. According to the calculation model for the effective thermal conductivity for a two-phase material [32], the overall thermal conductivity of LZ and LaOCl will be higher than that of a pure phase LZ, because the thermal conductivity of LaOCl is higher than that of LZ. Additionally, the difference in microstructures also results in changes in the thermal conductivity. As shown in Fig. 3c, the compound particles composed of lanthanum and oxygen are much larger than those obtained by the reverse dropping method. Large particles are not superior as thermal insulation compared to tiny powders [17,33] since small particles, especially nanoparticles, can provide more grain boundaries to scatter phonons.

4. Conclusion

We studied the synthesis process of LZ by two different coprecipitation–calcination methods. Adding reactants in a different order affects the product composition and structure; the natural dropping method and reverse dropping method produce precipitates with different compositions: a mixture of lanthanum hydroxide and zirconium hydroxide, and a –La–O–Zr– compound, respectively. These solids undergo different decomposition and crystallization routes. At about 850 °C, LZ with fluorite structure was synthesized, and LZ with pyrochlore structure can be obtained at 1000 °C by the reverse dropping method. The precipitates from the reverse dropping method can produce pure and highly crystalline LZ, while the product obtained by the natural dropping method is a mixture of LZ with a small amount of LaOCl.

Ceramics were prepared by subsequently sintering the powders at 1500 °C for 6 h. The thermal conductivity of the LZ specimen from the reverse dropping method was about half of that produced by the natural dropping method. The compositions and microstructures of the precipitates, along with the property of the second phase, are the main factors that should be responsible for the difference in thermal conductivity.

Acknowledgements

We gratefully acknowledge the help from Inorganic Materials Analysis and Testing Center of Shanghai Institute of Ceramics, Chinese Academy of Sciences. This work is supported in part by the Century Program (One-Hundred-Talent Program) of the Chinese Academy of Sciences for special funding support.

References

[1] N.P. Padture, M. Gell, E.H. Jordan, Science 296 (2002) 280–284.
[2] A.G. Evans, D.R. Clarke, C.G. Levi, J. Eur. Ceram. Soc. 28 (2008) 1405–1419.
[3] Z.G. Liu, J.H. Ouyang, Y. Zhou, J. Alloys Compd. (2008), doi:10.1016/j.jallcom.2008.05.053.
[4] R. Cremer, M. Witthaut, K. Reichert, M. Schierling, D. Neuschuetz, Surf. Coat. Technol. 108–109 (1998) 48–58.
[5] Z.H. Xu, L.M. He, R.D. Mu, X.H. Zhong, Y.F. Zhang, J.F. Zhang, X.Q. Cao, J. Alloys Compd. (2008), doi:10.1016/j.jallcom.2008.06.064.
[6] Z.G. Liu, J.H. Ouyang, B.H. Wang, Y. Zhou, J. Li, J. Alloy Compd. 466 (2008) 39–44.
[7] B. Saruhan, P. Francois, K. Fritscher, U. Schulz, Surf. Coat. Technol. 182 (2004) 175–183.
[8] W. Ma, S.K. Gong, H.B. Xu, X.Q. Cao, Surf. Coat. Technol. 200 (2006) 5113–5118.
[9] R. Vassen, X.Q. Cao, F. Tietz, G. Kerkhoff, D. Stoever, in: E. Lugscheider, P.A. Kammer (Eds.), Proceedings of the United Thermal Spray Conference'99 (Dusseldorf, Germany, March 1999), ASM Thermal Spray Society, Dusseldorf, Germany, 1999, pp. 830–834.
[10] W. Pan, Q. Xu, L.H. Qi, J.D. Wang, H.Z. Miao, K. Mori, T. Torigoe, Key Eng. Mater. 280–283 (2005) 1497–1500.
[11] Z.H. Xu, L.M. He, X.H. Zhong, R.D. Mu, S.M. He, X.Q. Cao, J. Alloys Compd. (2009), doi:10.1016/j.jallcom.2008.11.073.
[12] K. Bobzin, E. Lugscheider, N. Bagcivan, High Temp. Mater. Process. 10 (2006) 103–108.
[13] X.Q. Cao, R. Vassen, W. Jungen, S. Schwartz, F. Tietz, D. Stoever, J. Am. Ceram. Soc. 84 (9) (2001) 2086–2090.
[14] D. Chen, R. Xu, Mater. Res. Bull. 33 (3) (1998) 409–417.
[15] J. Wang, S.X. Bai, H. Zhang, C.R. Zhang, J. Alloys Compd. (2008), doi:10.1016/j.jallcom.2008.09.161.
[16] J. Nair, P. Nair, E.B.M. Doesburg, J.G. van Ommen, J.R.H. Ross, A.J. Burggraaf, F. Mizukami, J. Mater. Sci. 33 (1998) 4517–4523.
[17] C.G. Zhou, N. Wang, H.B. Xu, Mater. Sci. Eng. A 452–453 (2007) 569–574.
[18] X.Q. Ma, F. Wu, J. Roth, M. Gell, H.E. Jordan, Surf. Coat. Technol. 201 (2006) 4447–4452.
[19] A. Jadhav, N.P. Padture, F. Wu, E.H. Jordan, M. Gell, Mater. Sci. Eng. A 405 (2005) 313–320.
[20] T. Kawano, H. Imai, Cryst. Growth Des. 6 (4) (2006) 1054–1056.
[21] S.M. Wang, G.J. Zhou, M.K. Lu, Y.Y. Zhou, S.F. Wang, Z.S. Yang, J. Am. Ceram. Soc. 89 (9) (2006) 2956–2959.
[22] J.H. Adair, H.G. Krarup, in: J.A. Voight, T.E. Wood, B.C. Bunker, W.H. Casey, L.J. Crossey (Eds.), Better Ceramics Through Chemistry II, Proceedings of the Materials Research Society Symposium, vol. 432, Materials Research Society, Pittsburgh, PA, 1997, p. 101.
[23] N.M. Dibtseva, K.I. Kienskaya, V.V. Nazarov, Colloid. J. 63 (2) (2001) 150–153.
[24] P. Southon, Ph.D. Thesis, University of Technology, Sydney, 2000.
[25] H. Kido, S. Komarneni, R. Roy, J. Am. Ceram. Soc. 74 (2) (1991) 422–424.
[26] H. Otaki, H. Kido, T. Hoshikawa, M. Shimada, M. Koizumi, Nippon Seramikkusu Kyokai Gakujutsu Ronhunshi 96 (1988) 124–126.
[27] R.A. McCauley, Ph.D. Thesis, The Pennsylvania State University, University Park, PA, 1969.
[28] M.O.D. Jarligo, Y.S. Kang, A. Kawasaki, Key Eng. Mater. 317–318 (2006) 31–36.
[29] R. Vassen, X.Q. Cao, F. Tietz, D. Basu, D. Stoever, J. Am. Ceram. Soc. 83 (8) (2000) 2023–2028.
[30] W.D. Kingery, J. Am. Ceram. Soc. 38 (7) (1955) 251–254.
[31] J. Singh, D.E. Wolfe, R.A. Miller, J.I. Eldridge, D.M. Zhu, J. Mater. Sci. 39 (2004) 1975–1985.
[32] W.D. Kingery, in: J.E. Burke (Ed.), The Thermal Conductivity of Ceramic Dielectrics, Progress in Ceramic Science, vol. 2, Pergamon Press, New York, 1962, p. 181.
[33] R.S. Lima, B.R. Marple, Mater. Sci. Eng. A 485 (2007) 182–193.